www.jjgastro.com

Journal of Gastroenterology Research and Practice

Research Article

Open Access, Volume 3

Study on the mechanism of action of "Astragalus-Vespae Nidus" in the treatment of gastric cancer

Jiatong Liu[1,2,3]; Xiafei Qi[1,2,3]; Liuxiang Wang[1,2,3]; Peng Su[1,2,3]*

[1]Affiliated Hospital of Nanjing University of Chinese Medicine, Jiangsu, Nanjing 210029, China.

[2]Nanjing University of Chinese Medicine, Jiangsu, Nanjing 210029, China.

[3]Jiangsu Provincial Hospital of Chinese Medicine, Jiangsu, Nanjing 210029, China.

***Corresponding Author: Peng Su**

Affiliated Hospital of Nanjing University of Chinese Medicine, Jiangsu, Nanjing 210029, China.

Email: shupengsp@njucm.edu.cn

Received: Aug 10, 2023

Accepted: Sep 13, 2023

Published: Sep 20, 2023

Archived: www.jjgastro.com

Keywords: Gastric cancer; TCM treatment; Astragalus-Vespae Nidus; Network pharmacology; Molecular docking.

Abstract

Objective: To investigate the active ingredients of "Astragalus-Vespae Nidus" and its mechanism of action on gastric cancer based on the network pharmacology method.

Methods: The active ingredients of the drugs were obtained by database search and related literature review. Predicted targets for gastric cancer were obtained using public databases. Gene Ontology (GO) and Kyoto Encyclopedia of Genomics (KEGG) pathway enrichment analyses were performed. Constructed "drug-active ingredient-target-pathway" network diagrams, collected gene immune tissue images using the HPA database, and further collected gene expression data using the GEPIA database.

Results: There were 41 active ingredients and 90 targets of "Astragalus-Vespae Nidus" and the GO enrichment analysis involved 379 Biological Processes (BP), 340 Cellular Components (CC) and 536 Molecular Functions (MF); the KEGG pathway enrichment analysis screened 34 pathways related to gastric cancer, mainly cancer pathway, AGE-RAGE signaling pathway, etc.

Conclusion: The "Astragalus-Beehive" drug pair has anti-gastric malignant tumor effects. Human oncogene (TP53), protein kinase (SRC), recombinant human Mitogen-Activated Protein Kinase 1 (MAPK1) and Epidermal Growth Factor Receptor (EGFR) are potential targets of "Astragalus-Hive" in the treatment of gastric cancer. It is expected to provide possibility for basic experiments and theoretical support for clinical treatment.

Introduction

Gastric Cancer (GC) is a leading contributor to global cancer incidence and mortality [1]. Since the majority of patients with gastric cancer are diagnosed at advanced stages, they are not suitable for surgery and present with locally advanced or metastatic disease [2]. The use of traditional Chinese medicine provides more possibilities for the treatment of gastric cancer. Therefore, it is particularly urgent to explore the mechanism of TCM treatment of gastric cancer, find possible drug targets, and provide basis for clinical treatment.

"Drug pair" is the smallest unit prescription, which is guided by the classical theory of Chinese medicine and follows the compatibility law of the seven emotions of Chinese medicine. It is the link between single Chinese medicine and compound medicine. Astragalus is reputed as "the strength of qi". It is often used as the sovereign medicine in many TCM works such as Synopsis of the Golden Chamber and Treatise on Febrile Diseases. The Vespae Nidus was first recorded in the Shennong Classic of Materia Medica. It is flat in nature, shaped like a lotus canopy, light and flexible, and good at expressing itself. The "astragalus honeycomb" drug pair is mostly used to treat the "spleen defi-

ciency" syndrome in the clinical treatment of gastric cancer [3]. The Astragalus can raise the yang and sink, support the toxin and expel pus, assist the Vespae Nidus to attack the toxin and kill insects, dispel wind and relieve pain. The combination of the two works together to improve qi, firm the surface, and detoxify and disperse knots.

At present, the mechanism of action of "Astragalus-Vespae Nidus" in the treatment of gastric cancer is still unclear, therefore, the target of "apple" in gastric cancer is predicted through network pharmacology, further validated through public platform database, and subsequently validated through molecular docking. To provide a theoretical basis for further research on "Astragalus-Vespae Nidus".

Materials and methods

Drug main ingredients collection

The active ingredients were obtained by searching "Astragalus-Vespae Nidus" in Traditional Chinese Medicine Database and Analysis Platform (TCMSP) [4], The main components were obtained with the criteria of strong pharmacokinetic activity, Oral Bioavailability (OB) value ≥30% and Drug-Like (DL) ≥0.18. Review of relevant literature to supplement public databases for missing active ingredients. Supplementary data were screened by reviewing the literature, SwisstADME database [5] (http://www.swissadme.ch/).

Target prediction

The chemical formulae and smile formulae corresponding to the components were collected by using the Pubchem database [6] and the chemical specialized database of the Shanghai Institute of Organic Chemistry, Chinese Academy of Sciences [7]. (http://www.organchem.csdb.cn./). The aggregated results were entered into the Swiss Target Prediction database [5] (http://www.swisstargetprediction.ch/), and the type "Homo sapiens" was selected to collect the targets.

Collect the targets by using Using "gastric cancer" as the keyword, we entered the DrugBank database [8], DisGeNET v6.0 database [9], and GeneCards human gene database [10] (www.genecards.org) .

The combined and de-duplicated target data were analyzed using VENNY 2.1.0 online [11] (https://bioinfogp.cnb.csic.es/tools/venny/index.html) interactive software to obtain the "drug-gastric cancer" targets.

Protein-protein interactions

The Protein-Protein Interaction (PPI) network was constructed using the STRING online database [12] (https: //string-db.org/) to obtain the interaction relationships that exist between target proteins.

GO and KEGG Pathway

Bioinformatics online analysis was performed using the Metascape database [13], species "Homo sapiens", to create enrichment analysis maps. Observe the relationship between pathway and target interactions.

Critical protein gene validation

Gene expression profiling interaction analysis [14] (GEPIA http://gepia.cancer-pku.cn/index.html) was used to analyze the mRNA expression levels of key target proteins with the top 10 degree values. (The GEPIA database contains RNA sequencing data of common malignancy samples and normal samples from TCGA and GEO databases). The analysis was performed in terms of different cancer types, different pathological stages and differential expression of patients' survival and normal/pathological tissues.

Immunological tissue validation

The HPA database [15] (The Human Protein Atlas, https: //www.proteinatlas.org) was used to analyze the immunohistological structure of key gene proteins, compare the protein expression differences in normal gastric tissues and gastric cancer tissues, and obtain representative immunohistochemical staining images.

Molecular docking

The top 5 values of active ingredients were selected through the PDB database [16] and the crystal structures with high resolution and relatively complete structure were chosen. The crystals were preprocessed with Auto Dock Tools software to remove irrelevant ligands and non-protein molecules and formatted to set up Grid Boxes with ligands as the center, and molecular docking was performed using Autogrid to obtain binding energies.

Those with strong binding energy were selected and visualized using pymol software.

Results

Ingredients and gastric cancer effects target of "Astragalus-Vespae Nidus"

Using each database collection, after merging and de-weighting, we finally obtained 16 active ingredients of Astragalus membranaceus and 25 active ingredients of Beehive.

After combining and de-duplicating using each database, a total of 434 predicted therapeutic targets were collected for Astragalus, 3869 therapeutic targets for Apis mellifera and 1088 targets related to. After interaction analysis (Figure 1), there are 91 therapeutic targets for gastric cancer in Astragalus and 31 in Vespae Nidus, of which 15 are common to both Astragalus and Vespae Nidus.

Drug-component-target network construction

The drug-active ingredient-pathway network diagram was constructed using cytoscape 3.7.1 software (Figure 2). The nodes in the light blue square in the diagram are the gastric cancer disease targets, and the nodes in the purple hexagon are the active ingredients of Astragalus. The nodes in the yellow diamond are the active ingredients of Vespae Niduss. The more lines connected to the node, the greater the role of the node in the network action.

Figure 2 shows that the larger degree values are HQ11 (MOL000098-Quercetin), HQ12 (MOL000422-Kaempferol), HQ1 (MOL000378-7-O-methylisomucronulatol), HQ2 (MOL000392-Formononetin), HQ8 (MOL000354-Isorhamnetin) and FF18 (2R)-5,7-dihydroxy-2-phenylchroman-4-one.

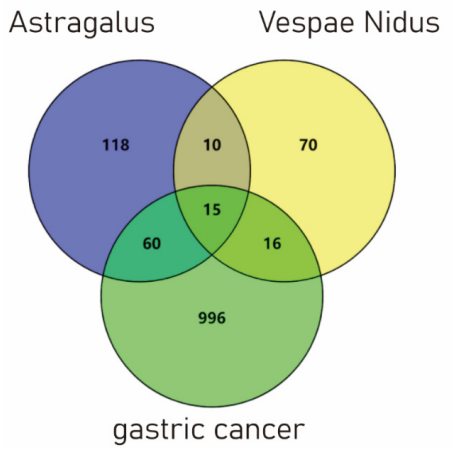

Figure 1: Drug and gastric canver target interaction chart. Blue represents Astragalus, yellow represents Vespae Nidus, green is gastric cancer target.

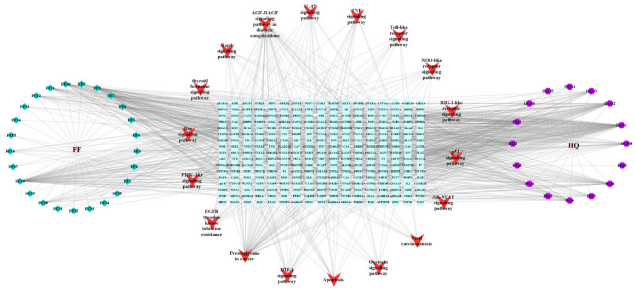

Figure 2: "Astragalus-Vespae Nidus"- target-pathway network diagram. The purple circcular node on the right side represents the astragalus component, the blue-green diamond node on the left side represents the hive component centered on the sky-blue square node represents the target site, and the red arrow node represents the pathway. The more nodes are connected, the greater the influence in the network.

Table 1: Detailed composition information of Astragalus-Vespae Nidus.

ID	MOL ID	NAME	OD	BL	Druglikeness	Chinese Medicine
HQ1	MOL000378	7-O-methylisomucronulatol	74.69	0.3		Astragalus
HQ2	MOL000392	Formononetin	69.67	0.21		Astragalus
HQ3	MOL000433	FA (6aR,11aR)-9,10-dimethoxy-6a,11a-dihydro-6H-benzofurano [3,2-	68.96	0.71		Astragalus
HQ4	MOL000380	c]chromen-3-ol	64.26	0.42		Astragalus
HQ5	MOL000211	Mairin	55.38	0,78		Astragalus
HQ6	MOL000371	3,9-di-O-methylnissolin	53.74	0,48		Astragalus
HQ7	MOL000239	Jaranol	50.83	0.29		Astragalus
HQ8	MOL000354	Isorhamnetin isomucronulatol-7,2'-di-O-	49.6	0.31		Astragalus
HQ9	MOL000439	glucosiole	49.28	0.62		Astragalus
HQ10	MOL000417	Calycosin	47.75	0.24		Astragalus
HQ11	MOL000098	Quercetin	46.43	0.28		Astragalus
HQ12	MOL000422	kaempferol	41.88	0.24		Astragalus
HQ13	MOL000296	Hederagenin 9,10-dimethoxypterocarpan-3-	36.91	0.75		Astragalus
HQ14	MOL000379	O---D-glucoside (3S,8S,9S,10R,13R,14S,17R)- 10,13-dimethyl-17-[(2R,5S)-5-propan-2-yloctan-2-yl]- 2,3,4,7,8,9,11,12,14,15,16,17- dodecahydro-1H-cyclopenta[a]phenanthren-	36.74	0,75		Astragalus
HQ15	MOL000033	3-ol	36.23	0.75		Astragalus
HQ16	MOL000387	Bifendate	31.1	0.75		Astragalus
FF1	MOL000579	Hydroquinone				Vespae Nidus
FF2	MOL002183	5-Propyl-2-thiouracil				Vespae Nidus
FF3	MOL000103	PHB				Vespae Nidus
FF4	MOL000414	Caffeate				Vespae Nidus
FF5		dTMP				Vespae Nidus
FF6	MOL002560	Chrysin				Vespae Nidus
FF7	MOL000006	Luteolin				Vespae Nidus
FF8	MOL002563	Galangin				Vespae Nidus
FF9	MOL000422	Kaempferol (2R)-5,7-dihydroxy-2-				Vespae Nidus
FF10	MOL000246	Phenylchroman-4-one				Vespae Nidus
FF11	MOL004576	Taxifolin				Vespae Nidus
FF12	MOL000513	3,4,5-trihydroxybenzoic				Vespae Nidus
FF13	MOL001801	Salicylic acid				Vespae Nidus

Protein-protein interaction

PPI network diagrams were obtained from STRING online data. The drug and gastric cancer intersection targets were taken and screened by taking twice the median value of Degree, and then selected by the median of Degree, Betweenness, and Closeness (Figure 3).

Obtained 26 core proteins in the PPI network. The top ten most core ones are: TP53, SRC, APP, MAPK1, EGFR, ESR1, AKT1, RB1, AR, RELA.

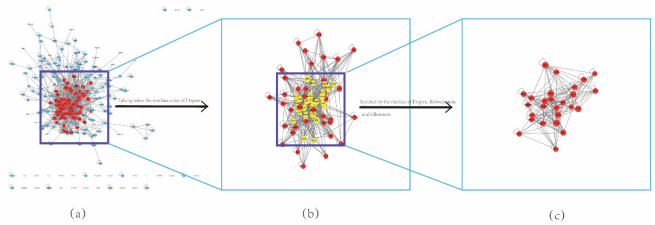

Figure 3: Protein-protein interaction.
(a) complete protein interaction graph with 273 nodes and 1038 connecting lines.
(b) Protein interaction map after screening with twice the median value of degree, with 70 nodes and 602 connecting lines.
(c) Protein interaction map with high centrality of targets after screening by greater than the median of degree, betweenness and and closeness. There are 26 nodes and 65 linkages.

KEGG and GO Pathway

The results showed that the most significant pathways were pathways in cancer, PI3K-Akt signaling pathway, FoxO signaling pathway, transcriptional misregulation in cancer, calcium signaling pathway, AGE-RAGE signaling pathway in diabetic complications, chemical carcinogenesis-receptor activation, and chemical carcinogenesis-reactive oxygen species (Figure 4).

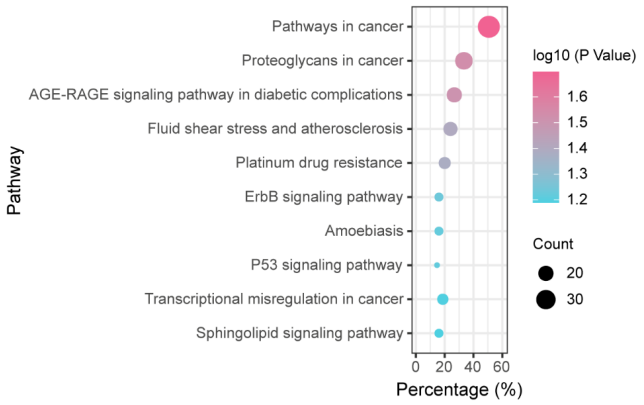

Figure 4: KEGG pathway enrichment analysis.

Table 2: KEGG Pathway.

GO	Category	Description	Count	%	-Log10 (P)	Log10(q)
hsa05200	KEGG Pathway	Pathways in cancer	77	32.49	75.01	-72.47
hsa05417	KEGG Pathway	Lipid and atherosclerosis	43	18.14	47.19	-44.95
hsa04933	KEGG Pathway	AGE-RAGE signaling pathway in diabetic complications	30	12.66	38.72	-37.02
hsa05207	KEGG Pathway	Chemical carcinogenesis-receptor activation	37	15.61	38.18	-36.54
hsa05208	KEGG Pathway	Chemical carcinogenesis-reactive oxygen species	37	15.61	37.32	-35.74
hsa04151	KEGG Pathway	PI3K-Akt signaling pathway	40	16.88	33.54	-32.08
hsa04068	KEGG Pathway	FoxO signaling pathway	25	10.55	26.83	-25.74
hsa05140	KEGG Pathway	Leishmaniasis	18	7.59	21.14	-20.3
hsa05202	KEGG Pathway	Transcriptional misregulation in cancer	24	10.13	21.13	-20.3
hsa04020	KEGG Pathway	Calcium signaling pathway	24	10.13	18.87	-18.14
hsa01524	KEGG Pathway	Platinum drug resistance	16	6.75	18.36	-17.64
hsa04931	KEGG Pathway	Insulin resistance	18	7.59	18.31	-17.6
hsa05221	KEGG Pathway	Acute myeloid leukemia	15	6.33	17.39	-16.72
hsa04024	KEGG Pathway	cAMP signaling pathway	18	7.59	12.7	-12.12
hsa04022	KEGG Pathway	cGMP-PKG signaling pathway	15	6.33	11.29	-10.75
hsa04725	KEGG Pathway	Cholinergic synapse	13	5.49	11.23	-10.7
hsa05216	KEGG Pathway	Thyroid cancer	9	3.8	11	-10.49
hsa04072	KEGG Pathway	Phospholipase D signaling pathway	14	5.91	10.88	-10.37
hsa00910	KEGG Pathway	Nitrogen metabolism	7	2.95	10.52	-10.02
hsa00140	KEGG Pathway	Steroid hormone biosynthesis	10	4.22	10.33	-9.84

GO enrichment analysis was performed using the metascape database (p<0.01) (Figure 5): 4588 enrichment results for Biological Process analysis (BP); 396 results for cellular component analysis (CC); and 613 results for Molecular Function analysis (MF).

The results of Go analysis showed that in Biological Process (BP), the main targets focused on foreign body stimulation, hormone, inorganic matter, lipopolysaccharide, oxygen level response, cell response to organic nitrogen compounds and lipids, positive regulation of cell migration, positive regulation of programmed cell death, negative regulation of cell population proliferation, positive regulation of protein phosphorylation, regulation of apoptosis signal pathway and apoptosis signal pathway, etc. In Cellular Components (CC), target actions are mainly focused on membrane rafts, vesicle lumen, transcriptional regulatory complex, nuclear membrane lumen, myelin sheath, axon, cytosol, membrane side, protein kinase complex, peroxisome, etc. In terms of Molecular Function (MF), target actions are focused on kinase binding, lipid binding, protein kinase activity, nuclear receptor activity, oxidoreductase activity, and prostaglandin receptor activity, etc.

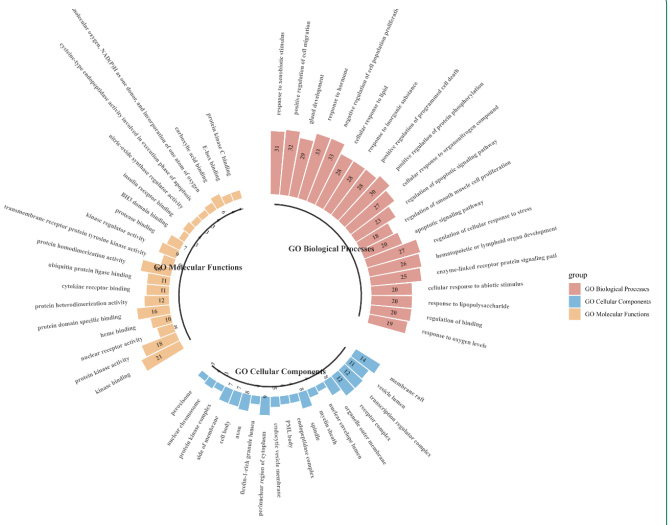

Figure 5: GO enrichment analysis. Flesh red bars represents Biological Process Analysis (BP), light blue bars Cellular Component Analysis (CC), and yellow bar Molecular Function analysis (MF). Longer bar lengths represent higher values of the corresponding bars.

Table 3: GO enrichment analysis.

GO	Category	Description	Count	%	Log10(P)	Log10(q)
GO:0045121	GO Cellular Components	Membrane raft	14	15.38	-11.95	-8.95
GO:0031983	GO Cellular Components	Vesicle lumen	11	12.09	-8.35	-5,56
GO:0005667	GO Cellular Components	Transcription regulator complex	12	13.19	-7.49	-4.93
GO:0043235	GO Cellular Components	Receptor complex	12	13.19	-7.05	-4.76
GO:0031968	GO Cellular Components	Organelle outer membrane	8	8.79	-6.28	-4,07
GO:0005641	GO Cellular Components	Nuclear envelope lumen	3	3.3	-5.5	-3.39
GO:0043209	GO Cellular Components	Myelin sheath	4	4.4	-4.98	-2,95
GO:0005819	GO Cellular Components	Spindle	8	8.79	-4.35	-2,41
GO:1905369	GO Cellular Components	Endopeptidase complex	4	4.4	-3.97	-2.06
GO:0016605	GO Cellular Components	PML body	4	4.4	-3.53	-1,68
GO:0030666	GO Cellular Components	Endocytic vesicle membrane	5	5.49	-3.51	-1.67
GO:0048471	GO Cellular Components	Perinuclear region of cytoplasm	9	9.89	-3.48	-1.67
GO:1904813	GO Cellular Components	Ficolin-1-rich granule lumen	4	4.4	-3.26	-1.48
GO:0030424	GO Cellular Components	Axon	8	8.79	-3.19	-1.45
GO:0044297	GO Cellular Components	Cell body	7	7.69	-2.86	-1.18
GO:0098552	GO Cellular Components	Side of membrane	7	7.69	-2.34	-0.74
GO:1902911	GO Cellular Components	Protein kinase complex	3	3.3	-2.22	-0.64
GO:0000228	GO Cellular Components	Nuclear chromosome	4	4.4	-2.19	-0.61
GO:0005777	GO Cellular Components	Peroxisome	3	3.3	-2.04	-0.53
GO:0009410	GO Biological Processes	Response to xenobiotic stimulus	31	34.07	-34.71	-30.52
GO:0030335	GO Biological Processes	Positive regulation of cell migration	32	35.16	-31.67	-27.79
GO:0048732	GO Biological Processes	Gland development	29	31.87	-31.48	-27.77
GO:0009725	GO Biological Processes	Response to hormone	33	36.26	-28.98	-25.74
GO:0008285	GO Biological Processes	Negative regulation of cell population proliferation	33	36.26	-28.38	-25.19
GO:0071396	GO Biological Processes	Cellular response to lipid	28	30.77	-27.19	-24.05
GO:0010035	GO Biological Processes	Response to inorganic substance	28	30.77	-26.77	-23.66

GO:0043068	GO Biological Processes	Positive regulation of programmed cell death	28	30.77	-26.27	-23.23
GO:0001934	GO Biological Processes	Positive regulation of protein phosphorylation	30	32.97	-25.17	-22.21
GO:0071417	GO Biological Processes	Cellular response to organonitrogen compound	27	29.67	-24.11	-21.27
GO:2001233	GO Biological Processes	Regulation of apoptotic signaling pathway	23	25.27	-23.27	-20.48
GO:0048660	GO Biological Processes	Regulation of smooth muscle cell proliferation	18	19.78	-22.32	-19.58
GO:0097190	GO Biological Processes	Apoptotic signaling pathway	20	21.98	-21.71	-19
GO:0080135	GO Biological Processes	Regulation of cellular response to stress	27	29.67	-21.61	-18.91
GO:0048534	GO Biological Processes	Hematopoietic or lymphoid organ development	26	28.57	-21.43	-18.75
GO:0007167	GO Biological Processes	Enzyme-linked receptor protein signaling pathway	25	27.47	-20.98	-18.33
GO:0071214	GO Biological Processes	Cellular response to abiotic stimulus	20	21.98	-20.37	-17.77
GO:0032496	GO Biological Processes	Response to lipopolysaccharide	20	21.98	-20.29	-17.74
GO:0051098	GO Biological Processes	Regulation of binding	20	21.98	-19.06	-16.6
GO:0070482	GO Biological Processes	Response to oxygen levels	19	20.88	-18.9	-16.47
GO:0019900	GO Molecular Functions	Kinase binding	21	23.08	-13.95	-10.27
GO:0004672	GO Molecular Functions	Protein kinase activity	18	19.78	-13.09	-9.71
GO:0004879	GO Molecular Functions	Nuclear receptor activity	8	8.79	-11.47	-8.57
GO:0020037	GO Molecular Functions	Heme binding	10	10.99	-10.84	-8.11
GO:0019904	GO Molecular Functions	Protein domain specific binding	16	17.58	-9.63	-7.1
GO:0046982	GO Molecular Functions	Protein heterodimerization activity	12	13.19	-9.43	-6.95
GO:0005126	GO Molecular Functions	Cytokine receptor binding	11	12.09	-9.19	-6.76
GO:0031625	GO Molecular Functions	Ubiquitin protein ligase binding	11	12.09	-8.77	-6.39
GO:0042803	GO Molecular Functions	Protein homodimerization activity	15	16.48	-8.67	-6.31
GO:0004714	GO Molecular Functions	Transmembrane receptor protein tyrosine kinase activity	6	6.59	-7.56	-5.27
GO:0019207	GO Molecular Functions	Kinase regulator activity	9	9.89	-7.31	-5.06
GO:0002020	GO Molecular Functions	Protease binding	7	7.69	-6.72	-4.6
GO:0051434	GO Molecular Functions	BH3 domain binding	3	3.3	-6.28	-4.22
GO:0005158	GO Molecular Functions	Insulin receptor binding	4	4.4	-6.27	-4.21
GO:0030235	GO Molecular Functions	Nitric-oxide synthase regulator activity	3	3.3	-6.04	-4.05
GO:0097200	GO Molecular Functions	Cysteine-type endopeptidase activity involved in execution phase of apoptosis	3	3.3	-5.66	-3.71
GO:0016709	GO Molecular Functions	Oxidoreductase activity, acting on paired donors, with incorporation or reduction of molecular oxygen, NAD(P)H as one donor, and incorporation of one atom of oxygen	4	4.4	-5.06	-3.18
GO:0031406	GO Molecular Functions	Carboxylic acid binding	6	6.59	-4.84	-2.99
GO:0070888	GO Molecular Functions	E-box binding	4	4.4	-4.83	-2.99
GO:0005080	GO Molecular Functions	protein kinase C binding	4	4.4	-4.63	-2.8

Gene supplement validation

The GEPIA database was used to analyze the differences in expression of key proteins in normal versus tumor tissues under different cancer species (Figure 6a). It could be seen that the key target proteins were significantly different in normal tissues versus tumor tissues. Subsequently, further validation showed that mRNA levels in TP53, SRC, APP, AKT1, RB1, and RELA were significantly downregulated in gastric cancer tissues compared with normal tissues (Figure 6b).

Further online analysis of the effect of key target protein expression on the survival of gastric cancer patients showed that the number of patients with survival greater than 70 months was significantly reduced except for EGFR low expression, and the number of patients with survival greater than 60 months was significantly increased for other proteins low expression (Figure 7a). And the protein expression also tended to change with tumor progression (Figure 7b). This online public database collected multiple clinical cases of protein expression to plot detailed box plots (Figure 7c). It was demonstrated that, except AR expression in tumor tissues was lower than that in normal tissues, the expression of other genes was significantly higher in tumor tissues, especially TP53, SRC, APP, MAPK1, RB1 were the most obvious.

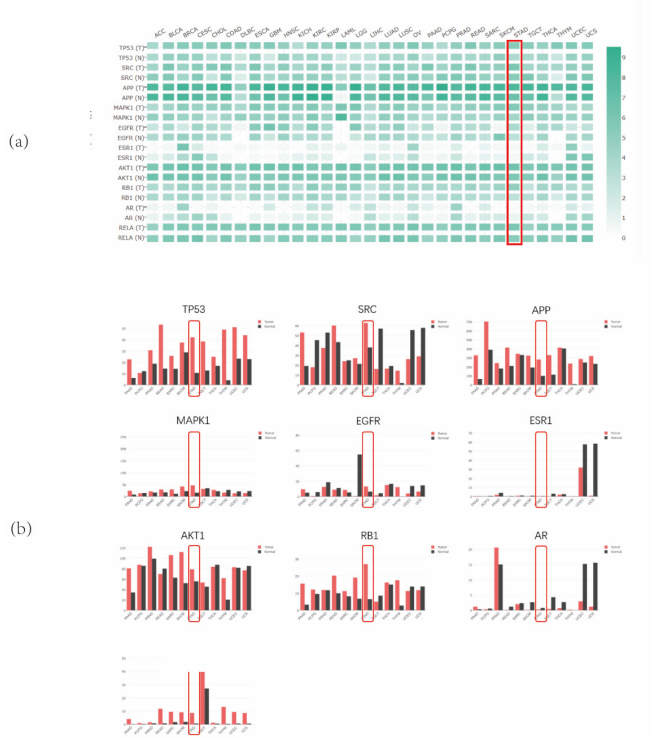

Figure 6: Protein Gene Expression **(a)** Differences in expression of key proteins in normal tissues and cancerous tissues (multi cancer types) and expression of target proteins in gastric cancer are shown in red.
(b) It is about the expression box diagram to see the indivudal protein expression morevisually.

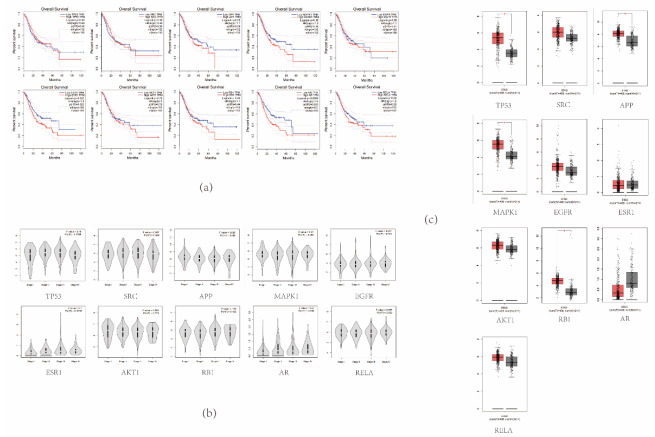

Figure 7: Differential expression of target proteins (univariate effects).
(a) Effect of high and low protein expression on patient survival.
(b) Differences in protein expression in different tumor stages.
(c) Differences in protein expression in normal and tumor tissues (detailed boxplot).

Histopathological analysis

Representative histopathological images were obtained using the online public database The Human Protein Atlas [15] (Human Protein Atlas proteinatlas.org). Figure 8 shows that the core targets were differentially expressed in normal gastric tissues except for AR and ESR1. TP53 and APP were significantly more expressed in tumor tissues than in normal gastric tissues, and SRC, MAPK1, and EGFR were significantly less expressed in tumor tissues than in gastric tissues (Figure 8).

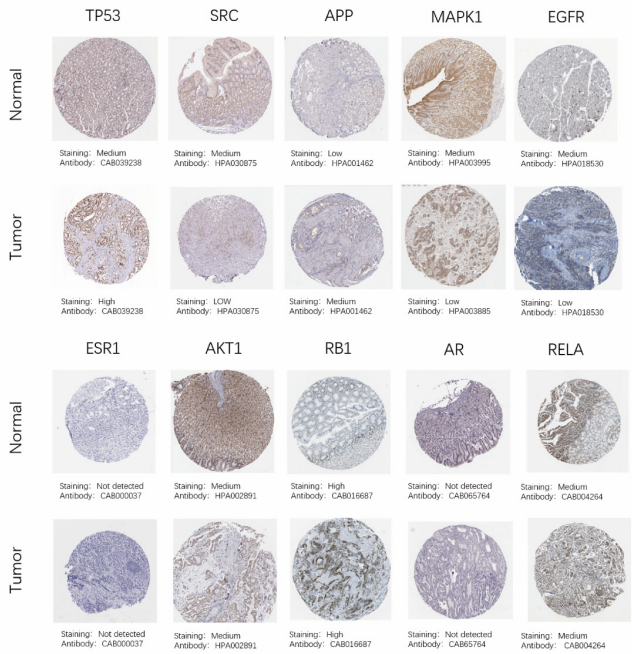

Figure 8: Histopathological expression. Comparison of normal tissue and tumor tissue sections.

Molecular docking verification

It is generally accepted that the lower the ligand-receptor binding energy, the more stable the conformation of the binding of ligand and receptor and the higher the possibility of binding. A docking score less than -4.25 can be considered as binding activity between the target and the component, a score less than -5.0 is better binding activity, and a score less than -7.0 is strong docking activity.

The five main active ingredients were molecularly docked to the top 10 protein targets of the enrichment analysis. The results showed that there were 28 active ingredients with binding energy less than -5 kJ/mol; 9 active ingredients less than -7 kJ/mol. The results showed that quercetin, formononetin, (2R)_5_7_dihydroxy_2_phenylchroman_4_one, Kaempferol, 7-O-methylisomucronulatol with SRC (PDB ID: 1US0[17]); MAPK1 (PDB ID: 2Y9Q[18]); ESR1 (PDB ID: 5UFX [19]); APP (PDB ID: 5OU0 [20]) had the good binding ability. PyMOL software was used to visualize and analyze the ones with a better binding ability (Figure 9). Complete molecular docking information plotted as a heat map (Figure 10).

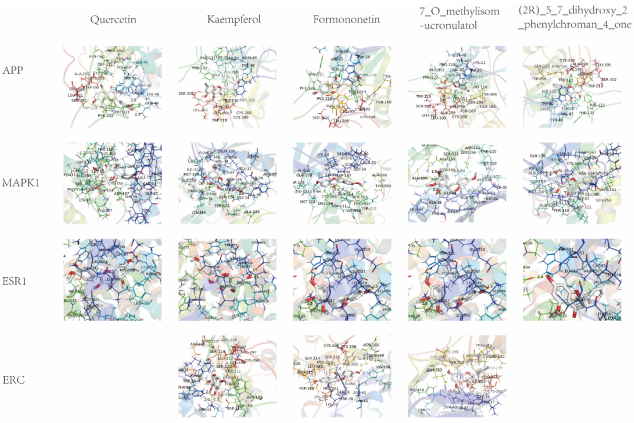

Figure 9: Detailed molecular docking diagram with summary results for docking energies >-7 kJ/mol.

Table 4: Detailed molecular docking data.

			Combined energy (KJ/mol-1)			
Target	Ligand	Quercetin	Formononetin	(2R)_5_7_ dihydrox y_2_phen ylchroma n_4_one	Kaempferol	7_O_methylisomucron ulatol.pdbqt_lizhenyu
P53(6GGC	EDO	-6,8	-4.7	-5.3	-5.3	-4.5
SRC(1US0)	NDP	-3,9	-9.2	-6.2	-6.6	-3,4
RELA(6TAN	MZN	-2,9	-2.9	-3.2	-3	-2.4
RB1(7D0E)	PEG	-3.3	-3	-3.3	-3.4	-3.9
APK1(2Y90	ANP	-8.3	-7.4	-8	-8.4	-6.3
ESR1(5UFX	86Y	-6,3	-7.1	-7,2	-6,5	-6.1
EGFR(5UG9	EDO	-6,3	-6.1	-6.2	-6	-5,8
AR(2QXW)	CIT	-4.8	-4.4	-4.8	-4.8	-4,4
APP(5OU0	AVT	-7.4	-7.3	-7.5	-7.2	-6.9
KT1(1UNC	4IP	-5.1	-4,7	-4.9	-5.1	-4.2

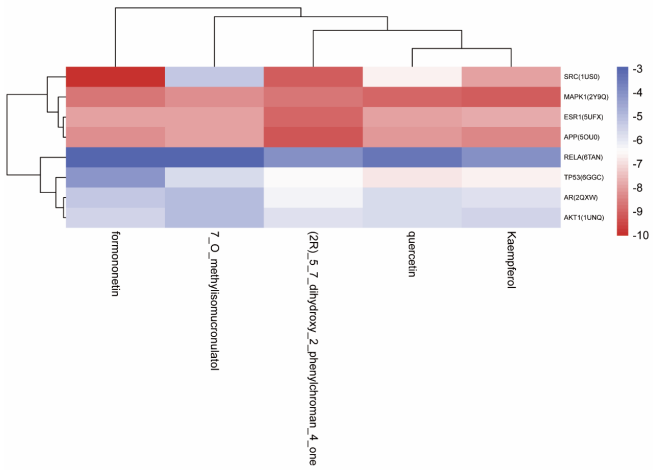

Figure 10: Complete molecular docking information.

Discussion

In this study, we analyzed the "Astragalus-Vespae Nidus" pair in terms of constituents and pathways of action and obtained the main constituents: quercetin, kaempferol, Formononetol, and isorhamnetin. The pathways associated with gastric malignancies were: Proteoglycans in cancer; p53 signaling pathway; Transcriptional misregulation in cancer; NF-kappa B signaling pathway; Chemical carcinogenesis.

The main components of the formula have been shown to have several anti-tumor and anti-inflammatory activities. Quercetin induces lysosomal activation and regulates ROS [21] synergistically leading to lipid peroxidation and iron death in tumor cells [22]. Quercetin affects changes in NF-κB activity[21], Notch/AKT/mTOR signaling pathway [23], PI3K/Akt/mTOR [24] mediating the regulation of anti-apoptotic proteins, including Bcl-2 and Bcl-xL. Kaempferol induces autophagic cell death via IRE1-JNK1 axis and HDAC/G9a pathway in gastric cancer [25]. For most cell types, Formononetin has been found to have concentration- and time-dependent effects on tumor proliferation [26-28]. The tumor-inhibitory effects of formononetin have been associated with the modulation of PI3K/AKT and STAT3 signaling pathways in both in vitro and in vivo models [29].

Cytoscape topological analysis of the protein PPI network yielded the network core proteins TP53, SRC, APP, MAPK1, EGFR, ESR1, AKT1, RB1, AR, and RELA. It is speculated that it may be the core target of the "Astragalus-Vespae Nidus" drug pair for the treatment of gastric cancer. *TP53* is the most frequent mutation in gastric cancer (GC) [30]. Dysregulation of the extracellular signal-Regulated Kinase/Mitogen-Activated Protein Kinase (ERK/MAPK) signaling pathway has been widely implicated in a range of human diseases, including cancers [31-33].

The online database was supplemented to demonstrate differential expression levels of target genes in gastric cancer/normal tissue, pathological stage, and patient survival. In addition, significant differential expression of the targets was confirmed in pathological tissues. Finally, molecular docking visualization analysis demonstrated that "Astragalus-Vespae Nidus" may be used to treat gastric cancer through these pathways.

Conclusion

In this study, the molecular mechanism of action of "Astragalus-Vespae Nidus" in the treatment of gastric cancer was constructed by using various public databases and software. The topological network involves multiple components, multiple targets, and multiple pathways with potential mechanisms of action, providing a theoretical reference for the treatment of gastric cancer with “Astragalus-beehive" drug pairs. Provide more possibilities for clinical treatment of gastric cancer with traditional Chinese medicine.

Declarations

Data availability statement: Datasets of gastric cancer targets generated during this study are available in DrugBank database and the DisGeNET database repository, [DrugBank database: https://go.drugbank.com/]. [DisGeNET database : https://www.disgenet.org].

The dataset of baicalein targets generated during this study is available in the TCMSP database, [https://tcmsp-e.com/].

The dataset of histopathological images in this study can be found in the HPA database, [https://www.proteinatlas.org/].

The protein conformation in this study can be found in the PDB database [https://www.rcsb.org/].

The gene expression levels in this study can be found in the GEPIA database, [http://gepia.cancer-pku.cn/].

Funding: This work was funded by the National Natural Science Foundation of China (nos. 81673918). Pilot GC project of clinical collaboration of traditional Chinese medicine and Western medicine on major difficult diseases in the state adminis-

tration of traditional Chinese medicine; the 2019" Construction Project of Evidence-based Capacity for Traditional Chinese Medicine" (2019XZZX-ZL003) in the state administration of traditional Chinese medicine; the open program of the third phase of the program of Traditional Chinese Medicine (TCM) Advantageous Subjects (ZYX03KF020); and the Science and Technology Project of Jiangsu Provincial Administration of Traditional Chinese Medicine (ZD201803).

Authors' contributions: Jiatong Liu Performed the experiments and drafted the manuscript; Xiafei Qi co-authored the experiments; Pei-Xing Gu performed the data analysis; Liu-Xiang Wang Completed animal experiments and data collection; Si-Yuan Song revised the manuscript; Xiaotao Niu Finish animal experiments; Peng Shu Conceived the experiments and designed the experiments.

References

1. Yeoh KG, P Tan. Mapping the genomic diaspora of gastric cancer. Nat Rev Cancer. 2022; 22: 71-84.
2. Kole C, et al. Immunotherapy for gastric cancer: A 2021 update. Immunotherapy. 2022; 14: 41-64.
3. Block KI, MN Mead. Immune system effects of echinacea, ginseng, and astragalus: A review. Integr Cancer Ther. 2003; 2: 247-67.
4. Ru J, et al. TCMSP: A database of systems pharmacology for drug discovery from herbal medicines. J Cheminform. 2014; 6: 13.
5. Daina A, O Michielin, V Zoete. SwissADME: A free web tool to evaluate pharmacokinetics, drug-likeness and medicinal chemistry friendliness of small molecules. Sci Rep. 2017; 7: 42717.
6. Kim S, et al. PubChem in 2021: New data content and improved web interfaces. Nucleic Acids Res. 2021; 49: D1388-d1395.
7. Shanghai Institute of Organic Chemistry of CAS. http://www.organchem.csdb.cn.
8. Wishart DS, et al. DrugBank 5.0: a major update to the DrugBank database for 2018. Nucleic Acids Res, 2018; 46: D1074-d1082.
9. Piñero J, et al. The DisGeNET knowledge platform for disease genomics: 2019 update. Nucleic Acids Res. 2020; 48: D845-d855.
10. Safran MRN, Twik M, BarShir R, Iny Stein T, Dahary D, et al. The GeneCards Suite Chapter, Practical Guide to Life Science Databases. 2022; 27-56.
11. Oliveros, J.C, Venny. An interactive tool for comparing lists with Venn's diagrams. Venny. An interactive tool for comparing lists with Venn's diagrams. 2007-2015.
12. Szklarczyk D, et al. The STRING database in 2021: Customizable protein-protein networks, and functional characterization of user-uploaded gene/measurement sets. Nucleic Acids Res. 2021; 49: D605-d612.
13. Zhou Y, et al. Metascape provides a biologist-oriented resource for the analysis of systems-level datasets. Nat Commun. 2019; 10: 1523.
14. Tang Z, et al. GEPIA: A web server for cancer and normal gene expression profiling and interactive analyses. Nucleic Acids Res. 2017; 45: W98-w102.
15. Uhlén M, et al. Proteomics. Tissue-based map of the human proteome. Science. 2015; 347: 1260419.
16. Berman HM, et al. The Protein Data Bank. Nucleic Acids Res. 2000; 28: 235-42.
17. Howard EI, et al. Ultrahigh resolution drug design I: Details of interactions in human aldose reductase-inhibitor complex at 0.66 A. Proteins. 2004; 55: 792-804.
18. Garai Á, et al. Specificity of linear motifs that bind to a common mitogen-activated protein kinase docking groove. Sci Signal. 2012; 5: ra74.
19. Fanning SW, et al. Specific stereochemistry of OP-1074 disrupts estrogen receptor alpha helix 12 and confers pure antiestrogenic activity. Nat Commun. 2018; 9: 2368.
20. Crespo I, et al. Design, synthesis, structure-activity relationships and X-ray structural studies of novel 1-oxopyrimido[4,5-c]quinoline-2-acetic acid derivatives as selective and potent inhibitors of human aldose reductase. Eur J Med Chem. 2018; 152: 160-174.
21. Ward AB, et al. Quercetin inhibits prostate cancer by attenuating cell survival and inhibiting anti-apoptotic pathways. World J Surg Oncol. 2018; 16: 108.
22. Wang ZX, et al. Quercetin induces p53-independent cancer cell death through lysosome activation by the transcription factor EB and Reactive Oxygen Species-dependent ferroptosis. Br J Pharmacol. 2021. 178: 1133-1148.
23. Soofiyani SR, et al. Quercetin as a Novel Therapeutic Approach for Lymphoma. Oxid Med Cell Longev. 2021; 2021: 3157867.
24. Ul Islam B, et al. Flavonoids and PI3K/Akt/mTOR Signaling Cascade: A Potential Crosstalk in Anticancer Treatment. Curr Med Chem. 2021; 28: 8083-8097.
25. Kim TW, et al. Kaempferol induces autophagic cell death via IRE1-JNK-CHOP pathway and inhibition of G9a in gastric cancer cells. Cell Death Dis. 2018; 9: 875.
26. Wang AL, et al. Formononetin inhibits colon carcinoma cell growth and invasion by microRNA-149-mediated EphB3 downregulation and inhibition of PI3K/AKT and STAT3 signaling pathways. Mol Med Rep. 2018; 17: 7721-7729.
27. Ye Y, et al. Formononetin-induced apoptosis of human prostate cancer cells through ERK1/2 mitogen-activated protein kinase inactivation. Horm Metab Res. 2012; 44: 263-7.
28. Yang Y, et al. Formononetin suppresses the proliferation of human non-small cell lung cancer through induction of cell cycle arrest and apoptosis. Int J Clin Exp Pathol. 2014; 7: 8453-61.
29. Ong SKL, et al. Focus on Formononetin: Anticancer Potential and Molecular Targets. Cancers (Basel). 2019; 11.
30. Park S, et al. Clinical Relevance and Molecular Phenotypes in Gastric Cancer, of TP53 Mutations and Gene Expressions, in Combination With Other Gene Mutations. Sci Rep. 2016; 6: 34822.
31. Yang X, et al. Long noncoding RNA GK-IT1 promotes esophageal squamous cell carcinoma by regulating MAPK1 phosphorylation. Cancer Med. 2022.
32. Roskoski R, Targeting ERK1/2 protein-serine/threonine kinases in human cancers. Pharmacol Res. 2019; 142: 151-168.
33. Ali ES, et al. ERK2 Phosphorylates PFAS to Mediate Posttranslational Control of De Novo Purine Synthesis. Mol Cell. 2020; 78: 1178-1191.e6.